

# Thick WC-12Co Coatings on Bearing Steel Fabricated by Low-Temperature High-Velocity Fuel Spray Process

Xu Jimin<sup>1</sup>, Zheng Wenying<sup>1</sup>, Zhang Juchen<sup>1,2</sup>, Zhang Cuiping<sup>3</sup>, Yuan Xiaoyang<sup>4</sup>

<sup>1</sup> Hefei University of Technology, Hefei 230009, China; <sup>2</sup> Nanjing University of Aeronautics & Astronautics, Nanjing 210016, China;

<sup>3</sup> Northwest Institute for Non-ferrous Metal Research, Xi'an 710016, China; <sup>4</sup> Key Laboratory of Education Ministry for Modern Design and Rotor-Bearing System, Xi'an Jiaotong University, Xi'an 710049, China

**Abstract:** High-velocity oxygen-fuel (HVOF) sprayed WC-12Co coating can improve system hardness and wear-resistance significantly. However, the coating will suffer from decarburization due to the high spray temperature and the large cooling rate in the HVOF process. With the application prospect of introducing thick WC-12Co coating into heavy-load rolling pairs to improve tribological performance and wear-resistance, such as the rolling bearing for thrust vector control in solid rocket engine, this study adopted a low-temperature high-velocity liquid fuel spray process to fabricate thick coatings on bearing steel. The results show that the modified process with a spray temperature around 1700 K is realized by the replacement of oxygen by oxygen-nitrogen mixed gas and the introduction of water-cooling system. Phase distribution, elementary composition, microstructure, bonding strength, elastic modulus and microhardness of coatings were investigated to verify the feasibility and advantage of the process. The bonding mechanism between the coating and the substrate is clarified. Based on experimental data and the assumption of the WC skeleton structure being filled with the cobalt phase, a simple formula of the microhardness of WC-12Co coating is proposed for theoretical predication and coating design.

**Key words:** HVOF; decarburization; thick WC-12Co coating; temperature-controllable; bonding mechanism; microhardness

Coating technology is an effective approach to modify the physical, chemical and mechanical properties of the substrate materials. Appropriate coatings can realize higher hardness, higher elastic modulus, lower friction coefficient and longer service life for some sliding/rolling contacting interfaces<sup>[1,2]</sup>. As a typical example, tungsten carbide-cobalt (WC-Co) coatings have been widely used in many cases, where they are subjected to severe friction and wear<sup>[3-5]</sup>. Thermal spraying is the commonest process of depositing WC-Co coating on a substrate, including air plasma spraying and high-velocity oxygen-fuel (HVOF) spraying. In particular, the featured high spray velocity of HVOF, realized by the Laval nozzle acceleration effect, can confer the designed thick-formed coatings a fairly dense microstructure and high bonding strength<sup>[6, 7]</sup>. Compared to some electrochemical processes, HVOF process can fabricate thick coating in a much shorter time and the

moderate spray temperature allows the fabrication of coating materials with a low or intermediate melting point<sup>[8]</sup>. However, a lot of evidences have shown that HVOF sprayed WC-Co coatings suffer from decarburization during the spraying process, which results in microstructure defects and a concomitant decrease in hardness<sup>[9]</sup>. It is proved that high temperature and large cooling rate are the main factors resulting in such phenomenon<sup>[10]</sup>. The existing studies show that sprayed WC-Co coating is subjected to complex chemical reactions. Part of WC is transformed into WC<sub>1-x</sub> and W<sub>2</sub>C and metallic tungsten, while another part is dissolved in the cobalt matrix to form M<sub>6</sub>C or M<sub>12</sub>C carbides<sup>[11]</sup>.

In order to improve the mechanical performance of WC-Co coating, a lot of studies based on process parameter modifications have been conducted. The adjustment of flame properties through different kinds of fuel can influence the hardness and

Received date: November 04, 2018

Foundation item: National Natural Science Foundation of China (51805131); China Postdoctoral Science Foundation (2018M640580); Fundamental Research Funds for the Central Universities (JZ2018HGBZ0155)

Corresponding author: Xu Jimin, Ph. D., Lecturer, School of Mechanical Engineering, Hefei University of Technology, Hefei 230009, P. R. China, Tel: 0086-551-62901359, E-mail: xujimin2017@hfut.edu.cn

Copyright © 2019, Northwest Institute for Nonferrous Metal Research. Published by Science Press. All rights reserved.

wear-resistance of HVOF sprayed coating to some extent<sup>[12, 13]</sup>. The HVOF equipment can be generally divided into three generations<sup>[14]</sup>. The third generation equipment usually uses liquid fuel instead of gas fuel used in the former two generations. The usage of gas fuel, such as propane and hydrogen, will cause some differences. The safety of gas fuel is poor and the pressure in combustion chamber must be controlled at a relatively low degree, which results in a lower spray velocity and a lower bonding strength. Compared to liquid fuel, gas fuel can make the combustion more complete and the spray temperature higher, which will cause a worse decarburization degree. Instead of pure oxygen, high-velocity air-fuel (HVOF) process adopts air as the combustion gas and its flame temperature is about 1000 K lower than that of HVOF<sup>[15]</sup>. The lower flame temperature can significantly suppress decarburization but the concomitant slower flame velocity will influence the bonding strength of the coating to the substrate. Wang et al<sup>[16]</sup> investigated the bonding strength of coatings under different substrate roughnesses and found that appropriate roughness can obtain higher bonding strength than well-polished surface. Ma et al<sup>[17]</sup> realized the improvement of coatings' mechanical properties and wear resistance by optimizing feedstock structure. Instead, some researchers replenished the post-heat treatment for sprayed coatings, such as sintering in an argon atmosphere<sup>[18]</sup> or carbon dioxide laser remolding<sup>[19]</sup>. Besides, some researchers tried to reveal the theoretical relationship between WC-Co coating microstructure and mechanical performance, which can provide some suggestions for coating fabrication. For example, there are several models available for hardness predication, such as reference energy model<sup>[20]</sup> and population model<sup>[21]</sup>. High hardness is attributed to the ultra-fine microstructure and alloy strengthening of the bonder phase<sup>[22, 23]</sup>. The finer the WC particle size, the higher the hardness of the coating.

With the application prospect of introducing sprayed WC-12Co coatings into heavy-load rolling friction pairs, such as the rolling bearings for thrust vector control in solid rocket engine, this study adopted a kind of low-temperature high-velocity fuel spray process to prepare thick coatings on bearing steel, which can suppress the above mentioned decarburization phenomenon to some extent. Except for water-cooling system, the process used the mixed gas of oxygen and nitrogen with a certain ratio as the oxidizer, which can easily realize the quantitative control of spraying temperature. Coating performance was investigated by some global characterization methods to reveal the advantages of modified spraying process. Additionally, the relationship between microhardness and coating microstructure was studied based on the measurement data, which can provide some suggestions for coating performance improvement.

## 1 Low-Temperature High-Velocity Fuel Spray Process

Firstly, it is necessary to discuss the reasons for fabricating

thick WC-12Co coatings instead of thin coatings. For some application sites with large external load, such as quintessential rotor-bearing system, thin WC-12Co coatings cannot fully exploit the advantage of high hardness. Additionally, modulus of WC-12Co coatings is much higher than that of common bearing steel<sup>[24]</sup>. According to the Hertz contacting theory, rolling friction coefficient  $\mu_f$  between two surfaces can be characterized as:

$$\mu_f \propto F_N \sqrt{\left( \frac{1-\nu_1^2}{E_1} + \frac{1-\nu_2^2}{E_2} \right)} \quad (1)$$

where,  $F_N$  is normal load,  $\nu_1$  and  $\nu_2$  are the Poisson's ratio, and  $E_1$  and  $E_2$  are elastic modulus of the contact surfaces.

Therefore, the introduction of high-modulus WC-12Co coatings is helpful to decrease friction coefficient and to improve tribological performance. But, if one of the surfaces has a thin coating, the compound elastic modulus  $E_c$  can be expressed as<sup>[25]</sup>:

$$\begin{cases} \frac{1}{E_c} = \frac{a_{\text{Bcc}}(t_f, a, h)}{E_f} + \frac{1 - a_{\text{Bcc}}(t_f, a, h)}{E_s} \\ a_{\text{Bcc}}(t_f, a, h) = \frac{2t_f}{\pi h \tan \varphi \left( 1 + \frac{2t_f}{\pi h \tan \varphi} \right)} \end{cases} \quad (2)$$

where,  $E_f$  and  $E_s$  are elastic modulus of the coating and substrate, respectively,  $t_f$  is thickness of coating,  $h$  is indentation or penetration depth,  $\varphi$  is the half-angle of the tip conical indenter at the maximum load, and  $a$  is contact radius.

If  $E_f > E_s$ , there is:

$$E_c - E_f = \frac{(1 - a_{\text{Bcc}})(E_f E_s - E_f^2)}{a_{\text{Bcc}} E_s + (1 - a_{\text{Bcc}}) E_f} < 0 \quad (3)$$

Thin coating systems cannot fully exploit the advantage of high elastic modulus either. Only a thick coating system with a high elastic modulus can realize a much lower rolling friction coefficient. It can be applied in some heavy-load rolling pairs, such as the rolling bearing for thrust vector control in solid rocket engine.

This study adopted a modified low-temperature high-velocity fuel spray system to fabricate thick WC-12Co coating samples based on HVOF spray system developed by Xi'an Hi-Tech Institute. The modified spray process is shown in Fig.1, which consists of fuel supply system, oxygen-nitrogen supply system, ignition system, water-cooling system and powder feed system. When spraying, a large amount of heat generated in combustion chamber is transmitted to the inner shell of the spray gun and influences the structural strength. Water-cooling system can relieve this problem and decrease the temperature of flame flow. Mixed gas of oxygen and nitrogen with a certain ratio is adopted as the oxidizer, which can control the spray temperature quantitatively. The mixture of aerosolized kerosene and oxidizer is ignited by spark plug into combustion chamber. Velocity of the fuel gas is accelerated to supersonic state through the Laval nozzle and the temperature is further decreased by the water-cooling system to suppress the decarburization degree as much as possible.

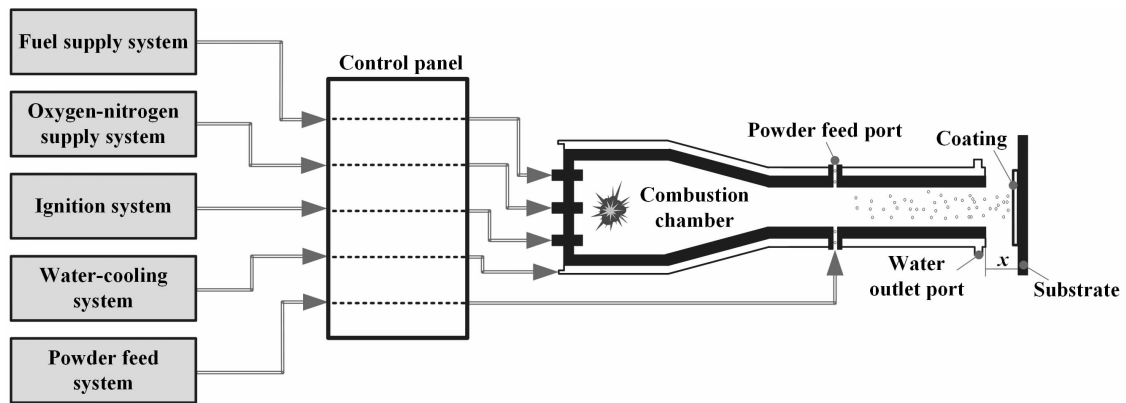


Fig.1 Structural scheme of low-temperature high-velocity fuel spray process

Precursor powders are fed by nitrogen in radial direction of the nozzle and the flow rate of nitrogen is  $0.4 \text{ m}^3 \cdot \text{h}^{-1}$ . The diameter of powder feed port is 4 mm. Therefore, the velocity of powder feed is about 8.8 m/s. The precursor WC-12Co powder is the compound of commercially available WC particles and Co particles in a certain ratio. The initial granularity of WC and Co is about 100 and 80 nm, respectively. Fig.2 shows the microstructure of precursor powders and the granularity is 15–45  $\mu\text{m}$  because of agglomeration.

According to some existing studies<sup>[26,27]</sup>, decarburization phenomenon of WC particles starts at about 1700 K. Theoretically, the decomposition temperature is about 1100 K but the degree can be ignored. Since lower spray temperature and concomitant decrease in spray velocity will weaken bonding strength, it is not rewarding to decrease spray temperature at that extent. In this study, the spray temperature of the outlet of the Laval nozzle was controlled around 1700 K through the water-cooling system. Flow rate of aerosolized kerosene, oxygen, nitrogen and precursor powders was set as  $6 \text{ L} \cdot \text{h}^{-1}$ ,  $20 \text{ m}^3 \cdot \text{h}^{-1}$ ,  $45 \text{ m}^3 \cdot \text{h}^{-1}$  and  $4 \text{ kg} \cdot \text{h}^{-1}$ , respectively. The spray distance  $x$  in Fig.1 was set as 100 mm. The substrate for coating spraying was conventional bearing steel and the surface roughness  $R_a$  was about 6.3  $\mu\text{m}$ .

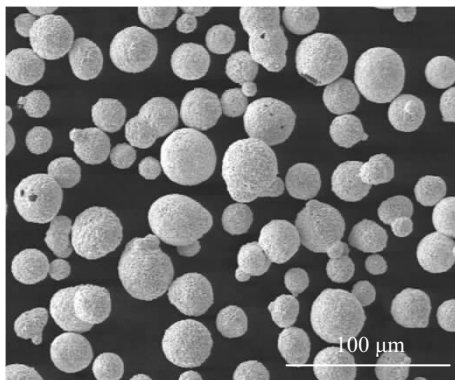


Fig.2 Microstructure of WC-12Co precursor powders (agglomeration state)

## 2 Results and Discussion

Using the above low-temperature high-velocity fuel spray process, 9 thick WC-12Co coating samples, named as a, b, c, d, e, f, g, h and i, were fabricated. Thickness of sample a, b and c is around 0.5 mm. Thickness of sample d, e and f is around 1 mm. Thickness of sample g, h and i is around 1.5 mm. Phase composition, elemental substance, microstructure, and hardness of samples were investigated by PW1700 X-ray diffraction instrument, JSM-6460 tungsten filament scanning electron microscope, SU-8010 field emission scanning electron microscope and MH-5L Vickers tester, respectively. Bonding strength between coating and substrate was detected by Instron 1195 electronic tensile testing device based on the tensile test standard C633-79 ASTM.

Fig.3 displays the XRD spectra of coating samples. The three prominent peaks and small peaks larger than  $60^\circ$  all correspond to WC phase. There is a small peak around  $40^\circ$  for several samples, which corresponds to the brittle  $\text{W}_2\text{C}$  phase. It is generated during the decarburization process of WC by two major reversible reactions<sup>[28]</sup>:



Compared to the XRD spectra in Ref.[9], undesirable phases in coating samples produced by temperature-controllable process are much less. The additional brittle phases can weaken the hardness and wear-resistance of coating samples.

Next, the detailed elemental composition of nine samples was analyzed by EDS. The test areas are about  $100 \mu\text{m} \times 200 \mu\text{m}$  and close to the bonding interface. Table 1 displays the testing data of the nine samples. The mass ratio of cobalt element ranges from 10.76 wt% to 13.73 wt%. Due to the agglomeration of precursor powders, the distribution of cobalt cannot be exactly uniform. The mole ratio between tungsten element and carbon element ranges from 0.94 to 1.14. When the value exceeds 1, it means that some WC powders are decomposed and carbon element escapes as  $\text{CO}_2$  gas. As a result,

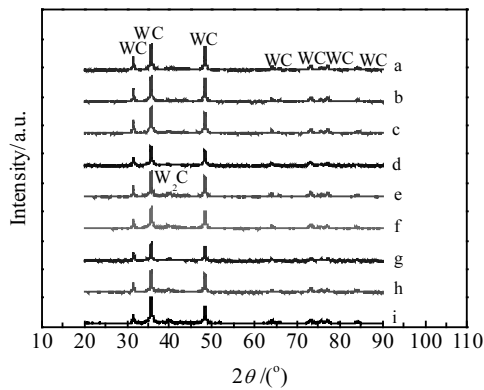
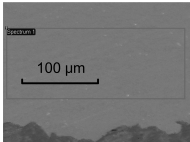


Fig.3 XRD patterns of nine WC-12Co coating samples

Table 1 Elemental composition of coating sample a~i

Testing area	Element	a	b	c	d	e	f	g	h	i
	W content/at%	41.30	40.28	39.11	40.87	42.97	40.99	41.20	41.90	42.15
	C content/at%	40.64	41.34	41.55	42.71	37.08	36.26	39.44	36.89	37.02
	W:C mole ratio	1.02:1	0.97:1	0.94:1	0.96:1	1.16:1	1.13:1	1.04:1	1.13:1	1.14:1
	Co content/wt%	11.64	12.06	12.92	10.76	12.35	13.73	12.42	13.31	13.03

Surface morphology of a WC-12Co coating sample and the bonding layer is displayed in Fig.4. Other samples possess similar characteristics. The magnification times are 40 and 2000. The structure of sprayed WC-12Co coating is very

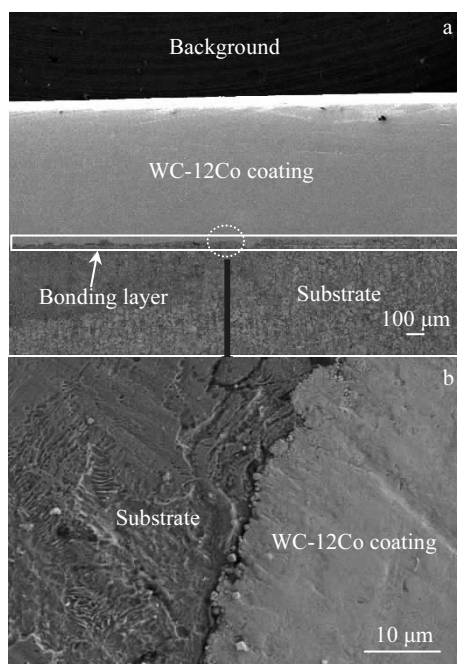


Fig.4 SEM micrographs of a coating sample (a) and its bonding layer between coating and substrate (b)

compounds with large W:C mole ratio are generated, such as  $W_2C$  or  $W_3CoC$ . The values of sample e, f, h and i are relatively large, which indicates that more undesirable brittle phases are generated in the testing areas. Compared to sample a, b and c, thickness of other six samples is larger. However, the testing areas are all close to the bonding interfaces. During spraying process, the late sprayed coating above the testing area will prevent the decrease of temperature in this area and deteriorate decarburization. The increase in coating thickness will make such insulating effect more obvious. Therefore, it can be deduced that more brittle phases are generated in the testing areas with the increase of coating thickness. The testing data basically agree with conclusion. The abnormal in sample d should be viewed as a random error of measurements.

compact and no obvious pores can be observed. The coating intrudes into the substrate and inosculates with each other, which confers the coating system a well bonding strength.

The melting point of WC particles is much higher than that of cobalt phase. When the precursor powders are transported to the high-speed high-temperature fuel gas, cobalt is in a molten state while WC particles are still in a solid state. When deposited on the substrate, WC hard particles can well disperse in the soft cobalt phase and the volumes among WC particles will be filled with cobalt. The bonding mechanism is realized by such kind of solid-liquid two-phase particle flow. As shown in Fig.5, the hard particles impact the substrate intensely and generate a large number of impacting craters. The liquid-state cobalt quickly fills these craters and adheres to the substrate tightly after solidification. The coating is gradually deposited on the substrate by repeating this process. Therefore, it is better to choose an appropriate surface roughness for substrate instead of well polishing. The bonding strength between coating and substrate increases with increasing the surface roughness within a certain range. Usually, it is not necessary to conduct special surface treatment except for cleaning. The bonding strength of coating samples was tested on an Instron 1195 electronic tensile testing device. The testing method is pull-off method, as shown in Fig.6. Compared to the tensile sample in standard measurements, the coating thickness is too small to be clamped. Usually, researchers use glue to fix the coating sample to the forcing device. Unfortunately, the bonding strength of WC-12Co coating samples is too large to

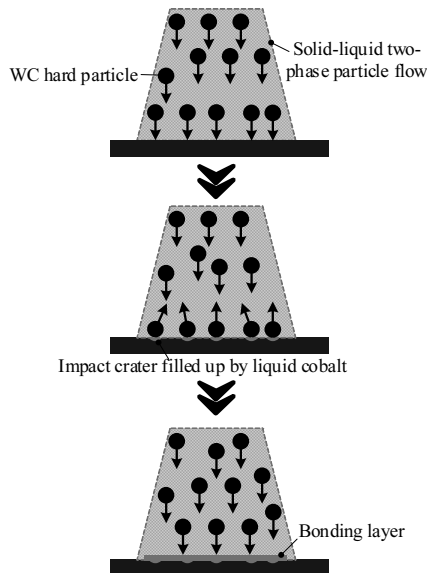


Fig.5 Deposition and bonding mechanism of WC-12Co coating system

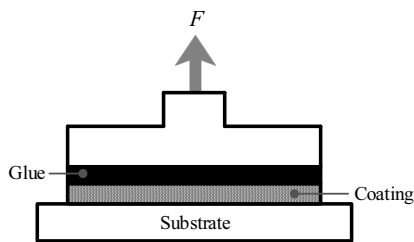


Fig.6 Schematic diagram for measuring bonding strength by pull-off method

find an appropriate glue. During measurements, the glue layer is destroyed before the coating. Therefore, we can only know that the bonding strength of these samples is higher than 70 MPa. The influence of coating thickness on bonding strength can be analyzed based on the data in Table 1. With the increase of coating thickness, more brittle phases will be generated around the bonding interfaces. As a result, the bonding strength will be weakened.

The elastic modulus of coating samples was measured by Knoop indentation method [29]. Each sample was measured three times. The average value of elastic modulus ranges from 270 GPa to 310 GPa, as shown in Fig.7. For conventional bearing steel, the elastic modulus is about 210 GPa. The introduction of thick WC-12Co coatings can significantly improve the system's ability to resist deformation, which is a positive factor in rolling tribological performance.

In particular, microhardness of coating samples was tested by indentation method with rhombus-type intender. The test load was set as 2.94 N (300 g) and each sample was measured ten times. The measured results are listed in Table 2 and Fig.8.

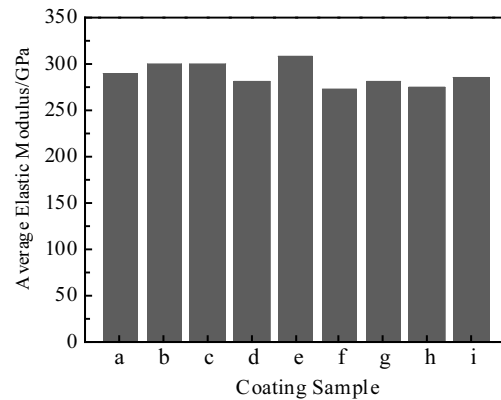


Fig.7 Average elastic modulus of coating samples

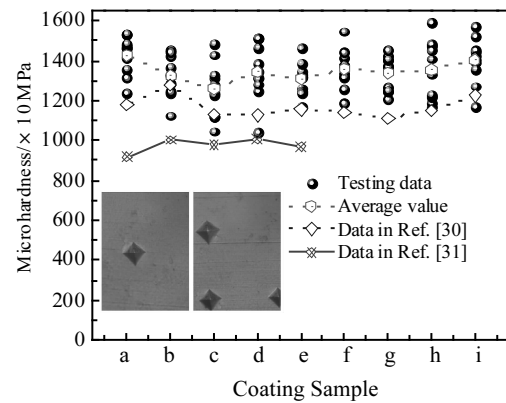


Fig.8 Microhardness of coating samples

The test data vary in a range of about 4000 MPa. For some indents, their edges are not angular and have some collapse phenomena. It is ascribed to some brittle phases or inward pores. The average microhardness values of nine coating samples are 14 290, 13 240, 12 600, 13 430, 13 100, 13 580, 13 410, 13 560 and 14 020 MPa. Generally, microhardness of common bearing steel is below 5000 MPa. High hardness of WC-12Co coating is beneficial for wear-resistance. Microhardness of WC-12Co coating samples fabricated by temperature-controllable high-velocity fuel spray process is about 1800 MPa, higher than that of hydrogen HVOF sprayed coatings reported in Ref.[30], which used the same testing method and parameters. Fig.8 also displays the microhardness of five coating samples from Ref.[31], which were prepared by propylene HVOF spray process. It can be clearly observed that the microhardness prepared by propylene HVOF spray process is the lowest. Although the temperature of the substrate during propylene HVOF spraying is maintained below 150 °C via compressed-air cooling system, the spray temperature of

flame should be quite large due to the complete combustion, which will result in severer decarburization. The testing results of  $W_2C$  contents in Ref.[31] also prove this point. As a result, microhardness is weakened significantly.

Therefore, it is an effective approach to suppress decarburization and improve mechanical performance by controlling the spray temperature. A relatively low spray temperature is beneficial for suppressing decarburization. Milman et al.<sup>[32]</sup> investigated the influence of spray temperature on coating hardness and obtained the similar conclusion that hardness decreases significantly with the increase of spray temperature. Ref.[26] reveals the decarburization mechanism of WC-12Co coatings. High spray temperature will allow a part of carbon to diffuse rapidly through the liquid and to get gasified at the particle surface by, e.g., the oxidative reaction  $2C+O_2 \rightarrow 2CO$  or  $2C+O_2 \rightarrow CO_2$ . As a result, WC phase will decompose and brittle phases are generated.

The existing studies<sup>[24, 33]</sup> have also shown that the particle size of precursor powders can influence coating performance significantly. In this study, we tried to investigate the quantitative relationship between WC particle size and microhardness by the experimental data. Firstly, the structure of WC-12Co coating was simplified as a WC skeleton structure

filled with cobalt phase. Two parameters were chosen as the main factors influencing microhardness, namely the mean grain size of WC particle in coating and the mean free path among WC particles. The microhardness values of WC and Co are 16 200 and 8250 MPa, respectively.

Grain size of WC particles and mean free path were analyzed by IMAGE-Pro-PLUS software. At first, the SEM photograph is binarized to determine the area of WC phase and Co phase, as shown in Fig.9. Polygon-shape WC particles are well dispersed in Co phase, which indicates that Co phase is in a completely molten state during spray process. The mean size of WC particles is smaller than that in Fig.2, which indicates that the agglomerated powders are scattered during high-speed spraying. Based on the binary photograph, the mean size of WC particles and mean free path are determined. The results are given in Table 3.

Through appropriate data fitting, a simple theoretical microhardness predication formula can be obtained, as shown in Eq.(6). It is not necessary to pursue the numerical accuracy of data fitting without limit. The fitting formula should take the existing experimental results into consideration, namely, the negative correlation between the microhardness and WC grain size.

**Table 2 Test results of microhardness of coating sample a-i ( $\times 10$  MPa)**

Test point	a	b	c	d	e	f	g	h	i
1	1465	1239	1313	1350	1264	1381	1403	1475	1573
2	1412	1246	1120	1316	1332	1322	1205	1173	1441
3	1359	1126	1124	1313	1350	1333	1380	1485	1391
4	1238	1423	1047	1511	1248	1419	1424	1410	1524
5	1478	1332	1487	1041	1240	1443	1267	1453	1171
6	1465	1455	1236	1386	1174	1186	1247	1332	1451
7	1537	1286	1283	1249	1390	1379	1370	1593	1273
8	1314	1444	1231	1283	1322	1258	1251	1190	1423
9	1536	1323	1330	1514	1320	1318	1408	1220	1360
10	1487	1370	1430	1467	1464	1548	1454	1232	1409

**Table 3 Theory predication results of microhardness**

Sample	Mean grain size/ $\mu m$	Mean free path/ $\mu m$	Measured microhardness/ $\times 10$ MPa
a	0.64	0.33	1429
b	0.70	0.36	1324
c	0.72	0.30	1260
d	0.68	0.30	1343
e	0.68	0.36	1310
f	0.67	0.30	1358
g	0.68	0.30	1341
h	0.71	0.30	1356
i	0.65	0.36	1402

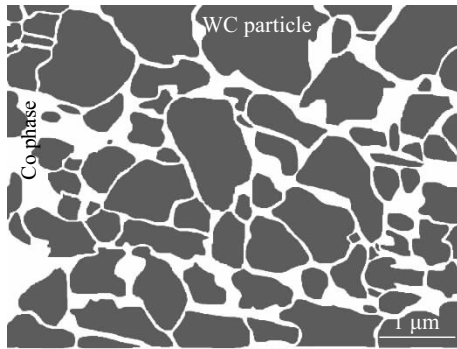


Fig.9 Binary treatment of SEM photograph for determining the area of WC phase and Co phase

$$\begin{aligned}
 H_{WC-12Co} &= \left( \frac{H_{WC}}{\sqrt{1+0.4d^2}} - H_{Co} \right) e^{-0.7 \cdot \rho} + H_{Co} \\
 &= \left( \frac{1620}{\sqrt{1+0.4d^2}} - 825 \right) e^{-0.7 \cdot \rho} + 825
 \end{aligned}
 \tag{6}$$

where,  $d$  ( $\mu\text{m}$ ) and  $\rho$  ( $\mu\text{m}$ ) are the mean grain size of WC particle in coating and the mean free path among WC particles, respectively. This formula can provide a simple tool for hardness predication and support coating design in some extent.

### 3 Conclusions

1) The modified process uses the mixed gas of oxygen and nitrogen instead of pure oxygen as the oxidizer in HVOF and water-cooling system to control the spray temperature at about 1700 K, which can realize the optimization of coating deposition speed and decarburization degree.

2) A few undesirable phases are generated during temperature-controllable spray process. The decrease of brittle phases is beneficial for high hardness and well wear-resistance.

3) During the spray process, WC particles are in a solid state while the cobalt is in a molten state. The hard particles impact the substrate and generate a large number of impacting craters. The liquid-state cobalt quickly fills them and adheres to the substrate tightly. Bonding mechanism of coating is realized by the effect of such solid-liquid particle flow. The bonding strength of fabricated coating samples is higher than 70 MPa.

4) The average elastic modulus of coating samples can reach about 290 GPa, much larger than that of common bearing steel. The introduction of thick WC-12Co coating into rolling pairs can decrease friction coefficient and enhance wear-resistance.

5) The average microhardness of coating samples ranges from 12 600~14 290 MPa, much higher than that of coatings fabricated by hydrogen HVOF process and propylene HVOF spray process. A simple formula for the theoretical microhardness predication of WC-12Co coating is proposed based on experimental data and the assumption that WC skeleton structure is filled with cobalt phase.

### References

- 1 Wang J L, Jia Q, Yuan X Y et al. *Applied Surface Science*[J], 2012, 258(24): 9531
- 2 Hardwicke C U, Lau Y C. *Journal of Thermal Spray Technology*[J], 2013, 22(5): 564
- 3 Zha B L, Gao S L, Yuan X J et al. *Rare Metal Materials and Engineering*[J], 2017, 46(2): 509 (in Chinese)
- 4 Ma N, Guo L, Cheng Z X et al. *Applied Surface Science*[J], 2014, 320: 364
- 5 Sahraoui T, Guessasma S, Jeridane M A et al. *Materials & Design*[J], 2010, 31(3): 1431
- 6 Jacobs L, Hyland M M, Bonte M D. *Journal of Thermal Spray Technology*[J], 1998, 7(2): 213
- 7 Jacobs L, Hyland M M, Bonte M D. *Journal of Thermal Spray Technology*[J], 1998, 8(1): 125
- 8 Vega J, Scheerer H, Andersohn G et al. *Corrosion Science*[J], 2018, 133: 240
- 9 Verdon C, Karimi A, Martin J L. *Materials Science & Engineering A*[J], 1998, 246(1-2): 11
- 10 Babu P S, Basu B, Sundararajan G. *Acta Materialia*[J], 2008, 56(8): 5012
- 11 Stewart D A, Shipway P H, McCartney D G. *Acta Materialia*[J], 2000, 48(7): 1593
- 12 Tillmann W, Vogli E, Baumann I et al. *Journal of Thermal Spray Technology*[J], 2008, 17(5-6): 924
- 13 Wang Y Y, Li C J, Ma J et al. *Transactions of Nonferrous Metals Society of China*[J], 2004, 14(S1): 72
- 14 Zha B L, Wang H G. *High-Velocity Oxygen-Fuel Spray Technology and Its Applications*[M]. Beijing: National Defense Industry Press, 2013: 1 (in Chinese)
- 15 Bolelli G, Berger L M, Borner T et al. *Surface and Coatings Technology*[J], 2015, 265: 125
- 16 Wang Y Y, Li C J, Ohmori A. *Thin Solid Films*[J], 2005, 485(1-2): 141
- 17 Ma N, Guo L, Cheng Z X et al. *Applied Surface Science*[J], 2014, 320: 364
- 18 Wang Q, Li L X, Yang G B et al. *Surface and Coatings Technology*[J], 2012, 206(19-20): 4000
- 19 Sheng T Y, Kong D J. *Tribology Transactions*[J], 2017, 60(5): 781
- 20 Šimůnek A, Vackář J. *Physical Review Letters*[J], 2006, 96(8): 85 501
- 21 Nourouzi S, Azizpour M J, Salimijazi H R. *Materials and Manufacturing Processes*[J], 2014, 29(9): 1117
- 22 Jia K, Fischer T E, Gallois B. *Nanostructured Materials*[J], 1998, 10(5): 875
- 23 Schubert W D, Neumeister H, Kingler G et al. *International Journal of Refractory Metals and Hard Materials*[J], 1998, 16(2): 133
- 24 Zha B L, Gao S L, Qiao S L et al. *Journal of Materials Engineering*[J], 2015, 43(4): 92
- 25 Puchi-Cabrera E S, Staia M H, Lost A. *Thin Solid Films*[J], 2015,

- 583: 177
- 26 Yuan J H, Zhang Q, Huang J et al. *Materials Chemistry and Physics*[J], 2013, 142(1): 165
- 27 Zhang Q, Yu L G, Ye F X et al. *Surface and Coatings Technology*[J], 2012, 206(19-20): 4068
- 28 Li C J, Ohmori A, Harada Y. *Journal of Materials Science*[J], 1996, 31(3): 785
- 29 Marshall D B, Noma T, Evans A G. *Journal of the American Ceramic Society*[J], 2010, 65(10): 175
- 30 Michael F, Itzhak R. *Surface and Coatings Technology*[J], 2000, 132(2-3): 181
- 31 Wang Q, Xiang J, Chen G Y et al. *Journal of Materials Processing Technology*[J], 2013, 213(10): 1653
- 32 Milman Y V, Luyckx S, Northrop I T. *International Journal of Metals & Hard Materials*[J], 1999, 17(1-3): 39
- 33 Coats D L, Krawitz A D. *Materials Science and Engineering A*[J], 2003, 359(1-2): 338

## 低温超音速火焰喷涂工艺制备轴承钢为基体的 WC-12Co 厚涂层

许吉敏<sup>1</sup>, 郑文颖<sup>1</sup>, 张聚臣<sup>1,2</sup>, 张翠萍<sup>3</sup>, 袁小阳<sup>4</sup>

(1. 合肥工业大学, 安徽 合肥 230009)

(2. 南京航空航天大学, 江苏 南京 210016)

(3. 西北有色金属研究院, 陕西 西安 710016)

(4. 西安交通大学 现代设计及转子轴承系统教育部重点实验室, 陕西 西安 710049)

**摘要:** 采用超音速火焰喷涂工艺 (HVOF) 制备的 WC-12Co 涂层能够显著提高系统的硬度和耐磨特性。然而, 该工艺中的高温参数会使得涂层在制备过程中产生脱碳现象。将 WC-12Co 涂层引入到滚动副中以提高界面的摩擦学性能和抗磨损特性, 例如固体火箭发动机中用于推力矢量控制的滚动轴承, 通过温度可控的超音速火焰喷涂工艺在轴承钢基体上制备涂层。详细研究了涂层的相分布、成分组成、微观结构、与基体的结合强度、弹性模量和显微硬度, 验证了改进后工艺的可行性和先进性, 并阐明了涂层与轴承钢基体之间的结合机制。在 WC 骨架假设和钴相均匀分布的假设下, 根据硬度的测试结果, 给出了 WC-12Co 涂层显微硬度的一个经验公式, 可用于涂层硬度的理论预估和设计优化。

**关键词:** 超音速火焰喷涂; 脱碳; WC-12Co 厚涂层; 温度可控; 结合机制; 显微硬度

---

作者简介: 许吉敏, 男, 1989 年生, 博士, 讲师, 合肥工业大学机械工程学院, 安徽 合肥 230009, 电话: 0551-62901359, E-mail: xujimin2017@hfut.edu.cn